

Artigo

Eta Model and CMIP5 Climate Change Projections for the São Francisco and Paraíba do Sul River Basins, Brazil

Greicy Kelly da Silva¹ , Antônio Duarte Marcos Júnior¹, Carlos Eduardo Sousa Lima¹, Marx Vinicius Maciel da Silva¹, Cleiton da Silva Silveira¹

¹*Departamento de Engenharia Hidráulica e Ambiental, Universidade Federal do Ceará, Fortaleza, CE, Brasil, Brasil.*

Recebido em: 17 de Dezembro de 2021 - Aceito em: 15 de Março de 2023

Resumo

O objetivo deste artigo é analisar as projeções de precipitação do modelo climático regional Eta para as bacias dos rios São Francisco (SF) e Paraíba do Sul (PS), Brasil. Para tanto, a resposta dinâmica da redução de escala foi discutida em comparação com os modelos CMIP5 e, em particular, com os modelos HadGEM2-ES e MIROC5 para o horizonte climático futuro de 2011 a 2040 em dois cenários do quinto relatório do Painel Intergovernamental sobre Mudanças Climáticas: RCP4.5 e RCP8.5. Os resultados indicam que o modelo Eta aninhado aos modelos globais representou adequadamente as simulações de precipitação para o clima presente. Quanto a avaliação da representação das projeções climáticas, as projeções Eta discordaram no sinal de mudança com seus forçantes GCMs e outros modelos CMIP5 nas bacias analisadas, amplificando o sinal mais seco. Reduções na precipitação foram apontadas para as duas bacias e com maior intensidade no cenário RCP8.5, variando em até -20% (SF) e 15% (PS) pelos modelos CMIP5 e em até quase -40% para os modelos Eta-HadGEM2-ES e Eta MIROC5 (SF e PS).

Palavras-chave: modelo atmosférico regional, ETA, climate changes, HadGEM2-ES, Bacia do Rio São Francisco.

Projeções de Mudanças Climáticas do modelo Eta e CMIP5 para as Bacias dos rios São Francisco e Paraíba do Sul, Brasil

Abstract

The aim of this article is to analyze the Regional Climate Model Eta precipitation projections for the São Francisco (SF) and Paraíba do Sul (PS) River basins, Brazil. For that, the dynamic downscaling response was discussed in comparison with the CMIP5 models and, in particular, with the models HadGEM2-ES and MIROC5 to future climate horizon 2011 to 2040 in two scenarios of the fifth report from Intergovernmental Panel on Climate Change: RCP4.5 and RCP8.5. The results indicate that the Eta model nested in the global models adequately represented the precipitation simulations for the present climate. As for the evaluation of the representation of climate projections, the Eta projections disagreed on the sign of change with their forcing GCMs and other CMIP5 models in the analyzed basins, amplifying the drier signal. Precipitation reductions were pointed out for the two basins and with greater intensity in the RCP8.5 scenario, ranging up to -20% (SF) and 15% (PS) by the CMIP5 models and up to almost -40% for the Eta-HadGEM2-ES and Eta MIROC5 (SF and PS).

Keywords: regional atmospheric model, ETA, climate changes, HadGEM2-ES, São Francisco River Basin.

1. Introduction

Global Climate Models (GCM) are widely used in the study of climate and its changes, projecting changes based on a set of anthropogenic forcing scenarios (Marengo *et al.*, 2012; Chou *et al.*, 2014; Moise *et al.*, 2015; Brasil, 2016; Giorgi, 2019; Pickler and Mölg, 2021). Changes

in radiative forcing, mostly caused by anthropogenic factors, have been identified as the main cause of these changes through significant emissions of carbon dioxide (CO₂) and other gases that contribute to the formation of the greenhouse effect (IPCC, 2013; PBMC, 2016; Silva *et al.*, 2020).

The Intergovernmental Panel on Climate Change (IPCC) is the main scientific body for the assessment of impacts associated with climate change - having been created by the United Nations Environment Program (UNEP) and the World Meteorological Organization (WMO) in 1988 (IPCC, 2013). Since its inception, the IPCC has been releasing Assessment Reports (AR) on climate change, disclosing projection scenarios (which include the present scenario, future scenarios, paleoclimate simulations and idealized simulations) - using Global Climate Models (GCM - General Circulation Model) - based on the emission of Greenhouse Gases (IPCC, 2013). However, so that the results of the various models can be compared, all simulations follow a pattern, from the input data to the simulations, through groups that cooperate with each other in the Coupled Models Intercomparison Project (CMIP), having a link with the World Climate Research Program (WCRP).

The fact that global climate models make use of different physical representations of processes, in a relatively low-resolution grid, introduces a certain degree of uncertainty in these future climate change scenarios and, consequently, in the assessment of vulnerability and impacts arising from it. Nevertheless, the low-resolution grid of global models limits the simulation of smaller spatial scale systems (Cruz *et al.*, 2017; Borges de Amorim and Chaffe, 2019; Pickler and Mölg, 2021). Thus, obtaining more detailed projections for a given region with a higher spatial resolution than that provided by a GCM is particularly useful for the studies of the impacts of climate change on the management and operation of water resources (PBMC, 2014; Valério and Fragoso Júnior, 2015; BRASIL, 2016). However, such uncertainties become greater in the case of regional models, as they are strongly dependent on the boundary conditions and the methods used to adapt the RCM variables to the lower spatial resolution of the GCM; thus, according to Pielke and Wilby (2012), large-scale weather errors in GCMs are not only absorbed by RCMs, but can be amplified, due to their higher spatial resolution. Furthermore, if the RCM is nested in just a few GCMs, the high-resolution scenarios do not cover the full range of projected changes that a larger number of GCMs would indicate as plausible futures, thus increasing the uncertainty of the results obtained (Hewitson *et al.*, 2014).

Chou *et al.* (2014), Adam *et al.* (2015) and Tejadas *et al.* (2016) recommend the application of regionalization techniques for the assessment of extreme events and better use of climate information from global projections of future climate in studies of regional impacts. The dynamic downscaling technique, which consists of forcing a Regional Climate Model (RCM - with smaller grid spacing) with GCM data (with larger grid spacing), is shown as an output for better representation of subgrid forcings, such as: topography, coastline, vegetation heterogeneity, among others that can reduce the uncertainties of their impacts on

the regional climate, since the scale of data from GCMs are generally incompatible with the scales required for impact studies (Solman, 2013; Chou *et al.*, 2014; Sales *et al.*, 2015; BRASIL, 2016; Oliveira *et al.*, 2017; Pickler and Mölg, 2021).

The Eta model, among the wide variability of existing RCMs, has been used by several authors and Brazilian entities to assess the impacts of climate change on different sectors of society (Chou *et al.*, 2012; Marengo *et al.*, 2012; Chou *et al.*, 2012; Chou *et al.*, 2014; Oliveira *et al.*, 2017; Dereczynski *et al.*, 2020; Farias *et al.*, 2020; Silva *et al.*, 2020). Brito *et al.* (2019), for example, showed that the bias of the HadGEM2-ES and Eta models are similar in most of the climatic extremes of precipitation indicators for the Amazon Basin - the HadGEM2-ES is a climate model participating in the CMIP5 (5th phase of the CMIP - Coupled Models Intercomparison Project). Eta performed better when simulating extreme rains. The authors naturalized, however, the effect of HadGEM2-ES simulations on the quality of Eta simulations, due to the different physical and dynamic structuring of the bases of both models, also recommending the use of other global models as a boundary condition for the Eta.

Zakhia *et al.* (2020) identified the reduction in monthly precipitation (RCP8.5, at the end of the 21st century), with the projections of the Eta-HadGEM2-ES model in the Ribeirão Jaguara Hydrographic Basin, in Minas Gerais. The greatest increase in monthly precipitation was observed in the RCP4.5 scenario, during the period 2041-2070, with the projections of the Eta-MIROC5 model. The largest monthly increases in average temperature occurred towards the end of the 21st century (2071-2099) for all models with the RCP8.5 scenario.

However, few studies have evaluated how the Eta regional model behaves in relation to its global forcings, a fact that may have neglected the uncertainty of climate change in the Northeast region, or even omitted a signal associated with the bias error of the regional atmospheric model which can interfere with the reading of information (PBMC, 2014; Giorgi, 2019). RCM simulations are often biased due to systematic errors (Piani *et al.*, 2010; Teutschbein and Seibert, 2010; Themeßl *et al.*, 2011). In this sense, several studies show that the climate change signal can present significant differences between the RCMs and their respective forcing GCMs due to effects of local forces (Di Luca *et al.*, 2012; Rummukainen, 2016).

Hence, the present study was motivated by the following research questions: how do the Eta projections behave in relation to their respective forcing GCMs in the São Francisco and Paraíba do Sul River basins? As for the evaluation of the representation of climate projections on a small scale, do the Eta projections agree on the sign of change with their forcing GCMs and other CMIP5 models in the analyzed basins? Therefore, the objective was to analyze the projections of the regional model Eta and

some global models CMIP5, for the basins of the São Francisco and Paraíba do Sul Rivers. Discussing, in particular, the response of dynamic downscaling to large-scale forcing, comparing precipitation projections between Eta and their respective global forcings (HadGEM2-ES and MIROC5) for scenarios RCP4.5 and RCP8.5.

2. Material and Methods

2.1. Study region

The study was developed for the Paraíba do Sul and São Francisco River basins (Fig. 1). These basins are strategically important for the country, as they serve several consumptive and non-consumptive uses, including: human consumption, irrigation, industry, energy generation, among others.

The São Francisco River, one of the largest Rivers in the country, acts as one of the most important sources of water for the entire Northeast region. The area of its basin is equivalent to about 7.5% of the total area of Brazil and partially covers the Federal District and six Brazilian states: Minas Gerais, Goiás, Bahia, Pernambuco, Alagoas and Sergipe. The São Francisco River basin interconnects

the Southeast and Northeast regions, in addition to being characterized by climatic and environmental diversity (CBHSF, 2016).

The interannual cycle of meteorological variables makes it possible to identify similar patterns between the climate of the Alto (Aw type, hot and humid with summer rains, according to the Köppen Climate Classification) and the Médio São Francisco (Aw predominant with BShw climate variation, semiarid). On the other hand, between the Sub-médio (BShw type, semi-arid) and Baixo São Francisco (predominantly AS, hot and humid, with winter rains), the latter with less precipitation intensity. In the Alto and Médio São Francisco, the rainier months occur from November to March and the drier months from May to September, which in turn correspond to the months of lower temperatures. At the end of the winter months, maximum evaporation occurs, which coincides with the month with the highest wind intensity and lowest relative humidity. The Sub-médio and Baixo São Francisco are milder regions, with a higher wind intensity and lower precipitation intensity, compared to the Alto and Médio São Francisco. The precipitation climatology shows that the months with heaviest rainfall occurs from January to April, for the Sub-médio São Francisco, and from March

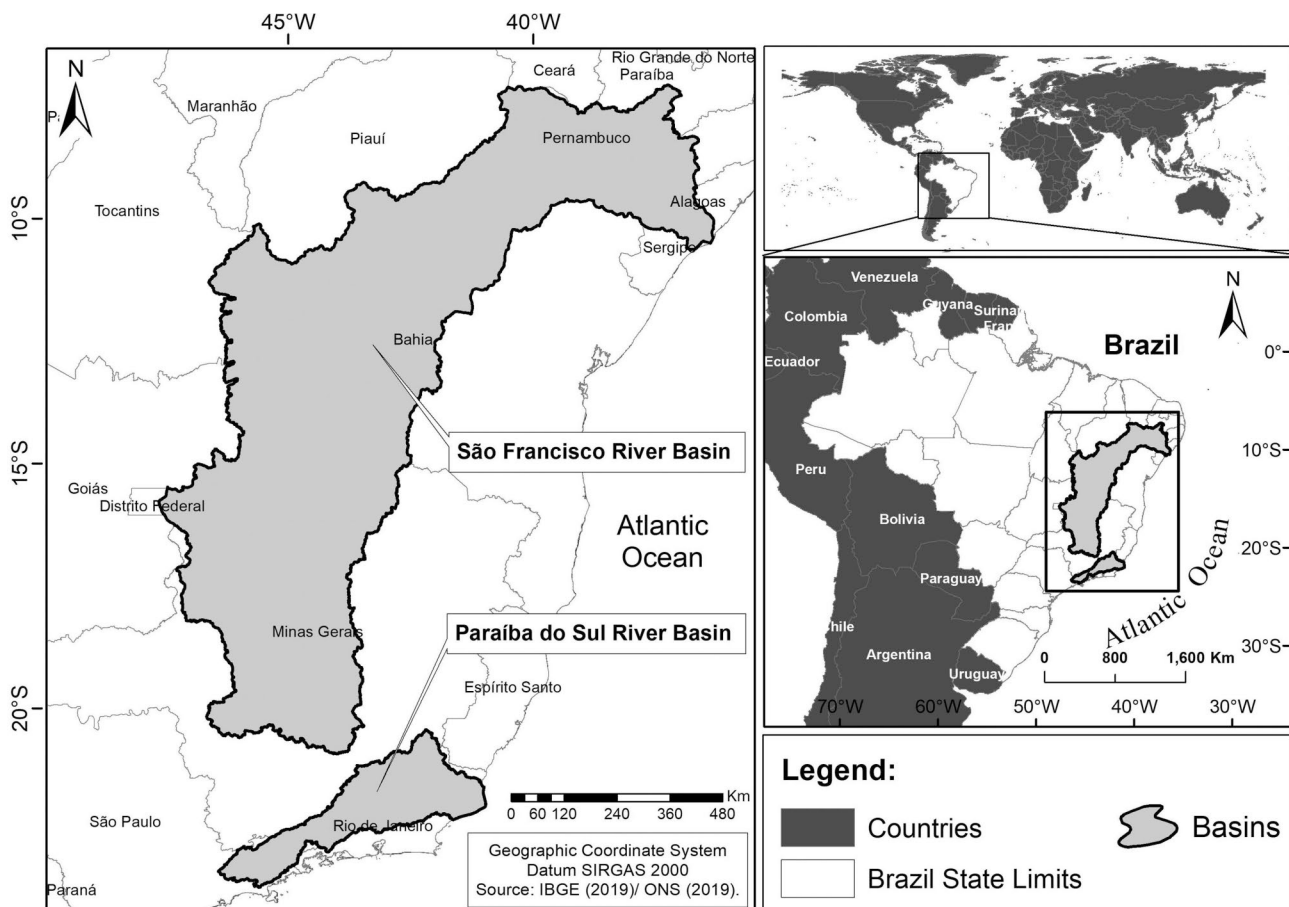


Figure 1 - Location map of the study region.

to August, for the Baixo São Francisco (CBHSF, 2016). The mean annual precipitation ranges from 1500 mm (Alto São Francisco) to 350 mm (Baixo e Médio São Francisco) (Bezerra *et al.*, 2019).

The Paraíba do Sul River basin, in turn, is located in the southeast region of Brazil (Fig. 1). According to the National Water Agency (2010) it has a drainage area of about 55,500 km² distributed across the states of São Paulo, Rio de Janeiro and Minas Gerais. The basin area corresponds to about 0.7% of the country's area and, approximately, to 6% of the Southeast region of Brazil. The region is characterized by a predominantly hot and humid tropical climate, with variations determined by differences in altitude and inflows of marine winds (CEIVAP, 2021). The Paraíba do Sul River basin has a tropical climate with an average annual temperature that varies between 18 °C and 24 °C. According to the detailed Köppen classification for Brazil (Alvares *et al.*, 2013), the climate basin is considered humid subtropical with dry winter and hot or temperate summer (Cwa or Cwb) in most of the basin, except the northwest region which is classified as tropical with dry winter (Aw). The rainfall regime is characterized by a dry period, which extends from June to September, and a very rainy period, which covers the months from November to January, when the great floods of the Paraíba do Sul River occur.

The highest rainfall occurs in the São Paulo section of the Serra do Mar, in the regions of the Itatiaia massif and its foothills and in the Serra dos Órgãos, a section of the Serra do Mar that accompanies the Região Serrana of the state of Rio de Janeiro, where the annual precipitation reaches exceeding 2000 mm. In these three high altitude regions, the average minimum temperatures reach less than 10 °C. The lowest rainfall occurs in a narrow strip of the center Paraíba do Sul and in the lower reaches of the basin (North and Northwest regions of Rio de Janeiro), with annual rainfall between 1000 mm and 1250 mm. Summer is characterized as rainy with accumulated precipitation between 200 and 250 mm/month. In winter, the driest period occurs, with accumulated rainfall of less than 50 mm/month (CEIVAP, 2021).

2.2. Climatic Data

2.2.1. Global-based projections

In this study, were used monthly precipitation data obtained from eighteen global climate models participating in the CMIP5 - an overview of CMIP5 and the experiment design can be found in Taylor *et al.* (2012). The Table 1 lists the models used in this study and their respective institutions and/or agencies and countries. The database comprised the monthly series from 1971 to 2005 (reference period) and from 2011 to 2040 was the period considered for the projections. No pre-processing of data from the GCMs described above was performed.

In this work, these projections are based on scenarios called Representative Concentration Pathways (RCP), published by the IPCC in the Fifth Assessment Report (AR5) and which represent the sets of projections of the components of anthropogenic radiative forcing, used as input data in the GCMs for climate and atmosphere chemistry modeling (IPCC, 2013). The possible scenarios for the end of the 21st century are: RCP 3.0-PD (Peak and Decline), with a peak in radiative forcing at 3 W/m² in the middle of the 21st century that decays to 2.6 W/m² until 2100, also known as RCP 2.6; RCP 4.5 with stabilization at 4.5 W/m² before the end of the 21st century; RCP 6.0 with stabilization at 6 W/m² after 2100; and RCP 8.5 with increasing path, reaching 8.5 W/m² in 2100 and 12 W/m² after the 21st century (Van Vuuren *et al.*, 2011; IPCC, 2013).

Only two global climate models (Table 2) had their results used as initial and contour conditions in the dynamic downscaling process for the Eta regional model. The choice of the two GCMs mentioned above is due to the fact that they are being commonly used in studies involving their global grid scale refinement.

The Hadley Center Global Environment Model version 2 - Earth System (HadGEM2-ES) is a grid-point model of resolution N96, which is approximately equivalent to 1.875 degrees in longitude direction and 1.275 degrees in latitude, and 38 levels in the atmosphere (Collins *et al.*, 2011; Martin *et al.*, 2011). In the ocean, the model has 40 levels in the vertical, and in the horizontal, the resolution varies from 1/3 degree in the tropics to 1 degree in latitudes higher than 30°. It is a model of earth system category with representation of the carbon cycle. Over land, the carbon cycle is modelled by the dynamic vegetation TRIFFID (Top-down Representation of Interactive Foliage Including Dynamics) (Cox, 2001). It distinguishes 5 plant functional types, broadleaf and needleleaf trees, C3 and C4 grass, and shrubs. The model includes atmospheric chemistry and aerosol model with organic carbon and dust representation (Collins *et al.*, 2011; Martin *et al.*, 2011).

The Model for Interdisciplinary Research on Climate version 5 (MIROC5) is a Japanese cooperatively developed model (Watanabe *et al.*, 2010). It is spectral in the atmospheric component with resolution T85, which is approximately 150 km in the horizontal, and has 40 vertical atmospheric levels. It is coupled to COCO 4.5 ocean model with 50 levels in depth and 1° of horizontal resolution. The radiative fluxes are calculated by a k-distribution scheme (Hasumi, 2007; Sekiguchi and Nakajim, 2008). The aerosol model, the SPRINTARS, is coupled to cloud microphysics scheme together with the radiation scheme, it uses the MATSIRO land surface scheme with 6 soil layers (Takata, Emori and Watanabe, 2003). Each grid box is formed by three tiles of potential vegetation, cropland, and lake. The scheme also contains

Table 1 - CMIP5 global models.

Model	Acronym	Responsible Institution or Agency / Country
1 Beijing Climate Center Climate System Model version 1.1	BCC-CSM1.1	Beijing Climate Center (BCC) and China Meteorological Administration (CMA) / China
2 Model for Interdisciplinary Research on Climate version5	MIROC5	Atmosphere and Ocean Research Institute, National Institute for Environmental Studies and Japan Agency for Marine-Earth Science and Technology / Japan
3 Hadley Center Global Environment Model version 2 - Atmosphere-Ocean	HadGEM2-AO	Met Office Hadley Centre / The United Kingdom
4 Community Climate and Earth-System Simulator Version 1.3	ACCESS1.3	ARC Centre of Excellence for Climate System Science / Australia
5 Commonwealth Scientific and Industrial Research Organization (version Mk3-6-0)	CSIRO-Mk3.6.0	Commonwealth Scientific and Industrial Research Organization in collaboration with Queensland Climate Change Centre of Excellence / Australia
6 Max Planck Institute - Meteorology - Earth System Model Medium Resolution	MPI-ESM-MR	Max Planck Institute for Meteorology / Germany
7 Community Climate and Earth-System Simulator Version 1.0	ACCESS1.0	ARC Centre of Excellence for Climate System Science / Australia
8 Model for Interdisciplinary Research on Climate - Earth System Model	MIROC-ESM	Atmosphere and Ocean Research Institute, National Institute for Environmental Studies and Japan Agency for Marine-Earth Science and Technology / Japan
9 Model for Interdisciplinary Research on Climate - Earth System Model Chemistry coupled version	MIROC-ESM-CHEM	Atmosphere and Ocean Research Institute, National Institute for Environmental Studies and Japan Agency for Marine-Earth Science and Technology / Japan
10 Max Planck Institute - Meteorology - Earth System Model Low Resolution	MPI-ESM-LR	Max Planck Institute for Meteorology / Germany
11 Community Earth System Model version 1-Bio-geochemistry	CESM1-BGC	National Science Foundation, Department of Energy, National Center for Atmospheric Research / The United States
12 Canadian Earth System Model (The second generation)	CanESM2	Canadian Centre for Climate Modelling and Analysis / Canada
13 Goddard Institute for Space Studies ModelE version 2 Russell	GISS-E2-R	Goddard Institute for Space Studies / The United States
14 Institut Pierre Simon Laplace - 5 Component Models version B - Low Resolution	IPSL-CM5B-LR	Institut Pierre Simon Laplace / France
15 Institut Pierre Simon Laplace - 5 Component Models version A - Low Resolution	IPSL-CM5A-LR	Institut Pierre Simon Laplace / France
16 Hadley Center Global Environment Model version 2 - Earth System	HadGEM2-ES	Met Office Hadley Centre / The United Kingdom
17 Institut Pierre Simon Laplace - 5 Component Models version A - Medium Resolution	IPSL-CM5A-MR	Institut Pierre Simon Laplace / France
18 Hadley Center Global Environment Model version 2 - Carbon Cycle	HadGEM2-CC	Met Office Hadley Centre / The United Kingdom

Table 2 - CMIP5 global models that acted as initial and boundary conditions for the RCM Eta.

Model	Resolution (degrees)		References
	Longitude	Latitude	
MIROC5	1.4008	1.40625	Watanabe <i>et al.</i> (2010)
HadGEM2-ES	1.25	1.875	Collins <i>et al.</i> (2011) and Martin <i>et al.</i> (2011)

River routing and the effects of snow on albedo. Sea ice thermodynamics and dynamics are represented (Watanabe *et al.*, 2010).

2.2.2. Regionally based projections

The regional climate model used was the Eta-CPTEC/INPE, as its dynamic downscaling simulations showed higher success rates than the predictions of the global models (Chou *et al.*, 2012; Marengo *et al.*, 2012). The Eta model is a grid point mesoscale model of primitive equations. The version of the Eta model that runs operationally at CPTEC/INPE is hydrostatic with a horizontal resolution of 40 km, in addition to another of 20 km, both with 38 layers in the vertical, and covering practically all of South America. Forecasts are provided twice a day, one with an initial condition at 00:00 UTC and the other at 12:00 UTC. The Eta regional model

(Mesinger *et al.*, 1988; Black, 1994) developed at the University of Belgrade. This model uses Arakawa's E grid (Arakawa and Lamb, 1977) and vertical coordinate η (Mesinger, 1984). Time integration uses the 'split-explicit' technique (Gadd, 1978). Turbulent processes are treated using the Mellor-Yamada scheme (1974). The long (Fels and Schwarzkopf, 1975) and short (Lacis and Hansen, 1974) radiation parameterization scheme was developed by the Geophysical Fluid Dynamics Laboratory. The model uses a modified Betts-Miller scheme to parameterize convection (Janjic, 1994). The surface schema is represented by the OSU schema (Chen *et al.*, 1997). In this work, the updated version of the Eta model is adapted for climate change studies. The sea surface temperature is taken from the global coupled ocean models: HadGEM2-ES and MIROC5, and it is daily updated. Initial soil moisture and soil temperatures are derived from the global models. Lateral boundaries are updated every 6 hours. The first year of integration is discarded from the analysis. The model was setup at 20 km resolution and 38 vertical levels. Model top is set at 25 hPa. The simulation area of the regional model was limited by the coordinates: 100° W-30° W; 30° N-50° S. The Eta model had its simulations obtained for the Historical, RCP4.5 (intermediate) and RCP8.5 (the one with very high GHG emissions -Greenhouse Gases) runs;

2.3. Observational data

The observed data used in this study was obtained from the Global Precipitation Climatology Centre (GPCC) and corresponds to precipitation climatology from 1971 to 2005, which provides global monthly precipitation data at a spatial resolution of 0.5° x 0.5° (Schneider *et al.*, 2015). The GPCC is a climate data center that provides global precipitation data. It uses rain gauge measurements collected from over 75,000 stations worldwide, along with additional satellite-based measurements, to create high-quality precipitation datasets. The GPCC offers monthly and daily precipitation data with a spatial resolution of 0.5° and 1.0°, respectively. The dataset covers the period from 1901 to present, making it a valuable source of long-term climate information. The GPCC data has been widely used in climate research, including in the evaluation and validation of climate models, the assessment of droughts and floods, and the analysis of climate variability and change (Schneider *et al.*, 2018).

2.4. Descriptive statistics

For validation between the observed data set and those from the Eta and CMIP5 models, a comparative analysis was performed based on a series of statistics described below, such as Mean, Median, Pearson Correlation Coefficient (R), Standard Deviation (SD) and Root of the Mean Square Error (RMSE).

The mean (\bar{x}) describes the sample of N values x_i that make up the series, as a single value that represents the center of the data distribution and the median acts as a measure of position and represents the value that is exceeded by 50% of the sample points. The SD, in turn, acts as a measure of dispersion, indicating the degree of uniformity of a sample's values around the mean - for more information and equations, see Wilks (2019).

In order to obtain a good precision indicator when correlating experimentally estimated and observed values, the Pearson Correlation Coefficient, also called correlation index, is used. Following the formulation adopted by Jolliffe and Stephenson (2003), Eq. (1) defines R as:

$$R = \frac{1}{N} \sum_{i=1}^N \left(\frac{\phi'_i \psi'_i}{\sigma_\phi \sigma_\psi} \right) \quad (1)$$

where ϕ'_i is the deviation from the estimated series and ψ'_i is the deviation from the observed series. Here, σ_ϕ and σ_ψ are also taken as the standard deviation of the averages of the estimated and observed series, respectively. Values of R for -1 and 1 refer to a perfect correlation, while the value of zero for R refers to no linear relationship between the studied variables (Moore, 2007).

According to Fox (1981) the RMSE is an error measure widely used in statistical treatment, as it presents a better sensitivity with regard to the growth of deviations between values. The *RMS* Error is computed through Eq. (2):

$$RMSE = \sqrt{\frac{1}{N} \sum_{i=1}^N (\phi_i - \psi_i)^2} \quad (2)$$

As the error measure is as close as possible to zero, it is said that there is greater similarity between the estimated and measured values.

In order to observe the quality of the climate models covered in this study, we chose to use the Taylor Diagram (DT) (Taylor, 2001), which provides a graphic summary of how close these models are to observational data. The DT increases the quality of the discussion about performance and the choice of a given model, as it is possible to simultaneously analyze a series of statistics from observed and estimated data (Pereira *et al.*, 2014). In this study, the DT was chosen with the three metrics mentioned above: the R, the SD and the RMSE.

2.5. Analysis techniques

The use of the analysis techniques described below is intended to compare the representation of the results of the Eta models with most of the CMIP5 GCMs. To evidence the existing divergence in the signal of change as well as to evaluate the spatial distribution of precipitation

anomalies in relation to its global forcings in the considered scenarios and in the analyzed basins.

2.5.1. Cluster analysis

To identify characteristics that evidence the existence of heterogeneity in the sign of changes proposed by the Eta models and the CMIP5 models, the cluster analysis (CA) technique was applied. In CA, the hierarchical agglomerative method proposed by Ward (1963) was considered, with the Euclidean distance squared as a dissimilarity measure (Jackson and Weinand, 1995; Lyra *et al.*, 2006; Lyra *et al.*, 2014). Ward's method forms groups, minimizing the dissimilarity or total sums of squares within groups. The Euclidean distance is the square root of the sum of the squares of the differences in values for each variable (Lyra *et al.*, 2006; Lyra *et al.*, 2014):

$$d_e = \left[\sum_{j=1}^n (P_{pj} - P_{kj})^2 \right]^{\frac{1}{2}} \quad (3)$$

where d_e is the Euclidean distance; P_{pj} and P_{kj} are the quantitative variables of individuals p and k , respectively. The choice of the number of clusters, although it may be random, was defined based on the average of similarity or internal dissimilarity of the obtained clusters, establishing a certain level that dictated the number of clusters.

2.5.2. Projections analysis

To obtain projections of precipitation of the GCM and RCM, the anomaly was calculated from the percentage change between the future values related to RCP4.5 and RCP8.5 scenarios and the historical average recorded for the Historical scenario, as expressed in Eq. (4):

$$A_{\text{annual}} = \frac{(P_{XXI}^a - P_{XX}^a)}{P_{XX}^a} \times 100 \quad (4)$$

where P_{XXI}^a is the annual precipitation variable of the projections for the 21st century scenarios and P_{XX}^a is the average annual precipitation for the 20th century.

3. Results

3.1 Precipitation validation analysis

Figure 2 presents the boxplot graph of the monthly average precipitation in the Paraíba do Sul and São Francisco River basins considering the GPCC data series for the period from 01/1971 to 11/2005. The Taylor Diagram HadGEM2 presented together provides a graphic summary of how close the climate models -ES and MIROC5 and the regional Eta forced by global models - hereinafter called Eta-HadGEM2-ES and Eta MIROC5, respectively - are to the observed data of the GPCC considering the variable precipitation.

It is observed in the Taylor diagrams that most models presented a strong correlation with the observed data, obtaining $R \geq 0.85$. In all basins, the Eta-HadGEM2-ES model showed the lowest SD values. Eta MIROC5, in turn, showed a SD in Paraíba do Sul closer to the SD of the set of observations. The MIROC5, despite showing a high correlation ($R \cong 0.99$), presented the highest values for the $RMSE$ (≥ 50 mm) and SD (> 100 mm). HadGEM2-ES had a good performance by showing R values above 0.95 and SD lower. In summary, in the Paraíba do Sul River basin, the correlation between the models and the observed data has values between 0.9 and 1.0.

With respect to seasonality, precipitations considered as discrepant (outliers) were identified in both basins. The low quartile 1 in both basins and the lowest median value in São Francisco are show in August, indicating that 25% of its precipitation data were close to zero and that 50% of these data were represented by a precipitation also around zero. In general, São Francisco showed a behavior with low variability from May to September. The highest 3rd and median quartiles were identified in December and January for São Francisco and Paraíba do Sul, respectively.

In San Francisco, specifically, a greater dispersion of precipitation data, also denounced by the greater occurrence of extremes or outliers was identified between the months of October and April. The interannual variations in rainfall in this region can be attributed to anomalies in the position and intensity of the intertropical convergence zone (ITCZ), caused by positive anomalies in the temperature of the Atlantic Sea surface, according to the study by Moura and Shukla (1981) and Nobre (1994), and by the occurrence of El Niño in the equatorial Pacific.

In Paraíba do Sul the months of September to March presented greater dispersion of precipitation data, due to by the greater occurrence of extremes or outliers. A greater variability of precipitation was identified for this basin. The action of the South Atlantic Convergence Zone (SACZ) is responsible for intense and persistent periods of precipitation, as well as reduced rainfall in the surroundings (Santana, 2021).

In the analysis of precipitation validation, the patterns of the Eta models and their global forcings showed values of strong correlation with the observed data, especially for the Eta-HadGEM2-ES, HadGEM2-ES and MIROC5 models. Allied to this, the Eta-HadGEM2-ES showed the lowest standard deviation values in the two basins. Chou *et al.* (2017) also obtained a good ability of the Eta model simulations forced by the HadGEM2-ES and MIROC5 data for the present climate (1961-1990) to reproduce the seasonality of rainfall for South America.

As for seasonality, the observed source of data indicated in the Paraíba do Sul River basin a greater variability in terms of precipitation when compared to the São Francisco River basin. This showed a behavior with low varia-

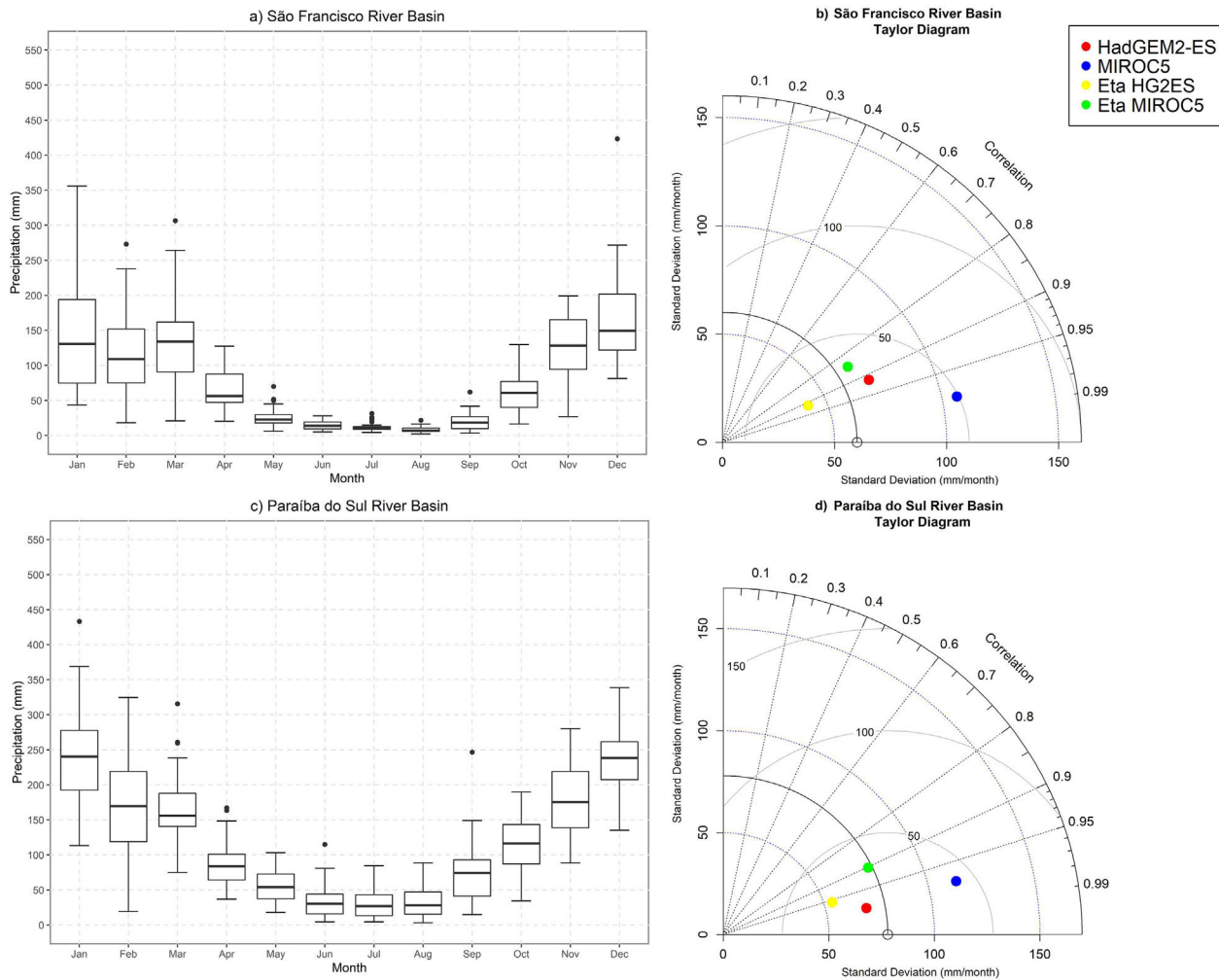


Figure 2 - GPCP monthly average rainfall boxplot for the period from 01/1971 to 11/2005 in a) São Francisco; Taylor diagram for the Eta-HadGEM2-ES, Eta MIROC5, HadGEM2-ES and MIROC5 models in relation to observed precipitation of the GPCP in b) São Francisco. The empty circle on the abscissa axis represents the set of observations; GPCP monthly average rainfall boxplot for the period from 01/1971 to 11/2005 in c) Paraíba do Sul and Taylor diagram for the Eta-HadGEM2-ES, Eta MIROC5, HadGEM2-ES and MIROC5 models in relation to observed precipitation of the GPCP in d) Paraíba do Sul. The empty circle on the abscissa axis represents the set of observations.

bility from May to September, which may be associated with the dry period in the Basin. The highest median values were identified in December and January for São Francisco and Paraíba do Sul, respectively.

3.2 Cluster analysis

The characterization of differences in models was explored in more detail using cluster analysis. Figure 3 shows the dendrograms obtained by Ward's hierarchical agglomerative method the percentage anomaly data of the average annual precipitation for the years 2011 to 2040 of the Eta-HadGEM2-ES and Eta MIROC5 models and the sixteen CMIP5 models in the São Francisco and Paraíba do Sul River basins in the RCP4.5 and RCP8.5 scenarios.

It is observed that models from the same institute have a smaller distance than other models and, therefore,

tend to be grouped closer together. The similarity level is very similar to model pairs that have many more common components. For example, the level of similarity between (i) MIROC-ESM-CHEM and MIROC-ESM and (ii) IPSL-CM5A-MR and IPSL-CM5B-LR. A greater dissimilarity was identified between some sets of models from the same institution, for example, the dissimilarity observed between (i) MIROC5 and MIROC-ESM / ESM-CHEM and (ii) IPSL-CM5A-LR and IPSL-CM5A-MR / IPSL-CM5B-LR.

It is interesting to note that the Eta-HadGEM2-ES model presented the largest Euclidean distance found from the rest of the model sample in both scenarios in Paraíba do Sul and in scenario RCP8.5 in São Francisco (and less markedly in RCP4.5), revealing a greater dissimilarity regarding the precipitation anomaly in relation to the other groups of models. Eta MIROC5, in turn, also showed a

level of dissimilarity regarding the homogeneous groups formed. But it has established itself with the family of the MIROC-ESM / ESM-CHEM model set in most scenarios and basins.

From the analysis of the dendrograms shown in Fig. 3, it was observed that models from the same institute tend to be grouped closer together and that a level of similarity was obtained very similar to the pairs of models that have much more common components - similar patterns were obtained in some studies from different parts of the globe (Mizuta *et al.*, 2014; Gibson *et al.*, 2017; Pathak *et al.*, 2019). The Eta-HadGEM2-ES model revealed a greater dissimilarity in terms of precipitation anomaly in

relation to the other groups of models. Eta MIROC5 also showed a level of dissimilarity with respect to homogeneous groups, but established itself with the family of the MIROC-ESM / ESM-CHEM model set in most scenarios and basins. It is noteworthy that the dissimilarity identified between some sets of models from the same institution may be associated with changes in atmospheric components during the model development process (Pathak *et al.*, 2019).

3.3. Projections analysis

In the analysis of the average percentage rainfall anomaly, the CMIP5 models indicate projections with

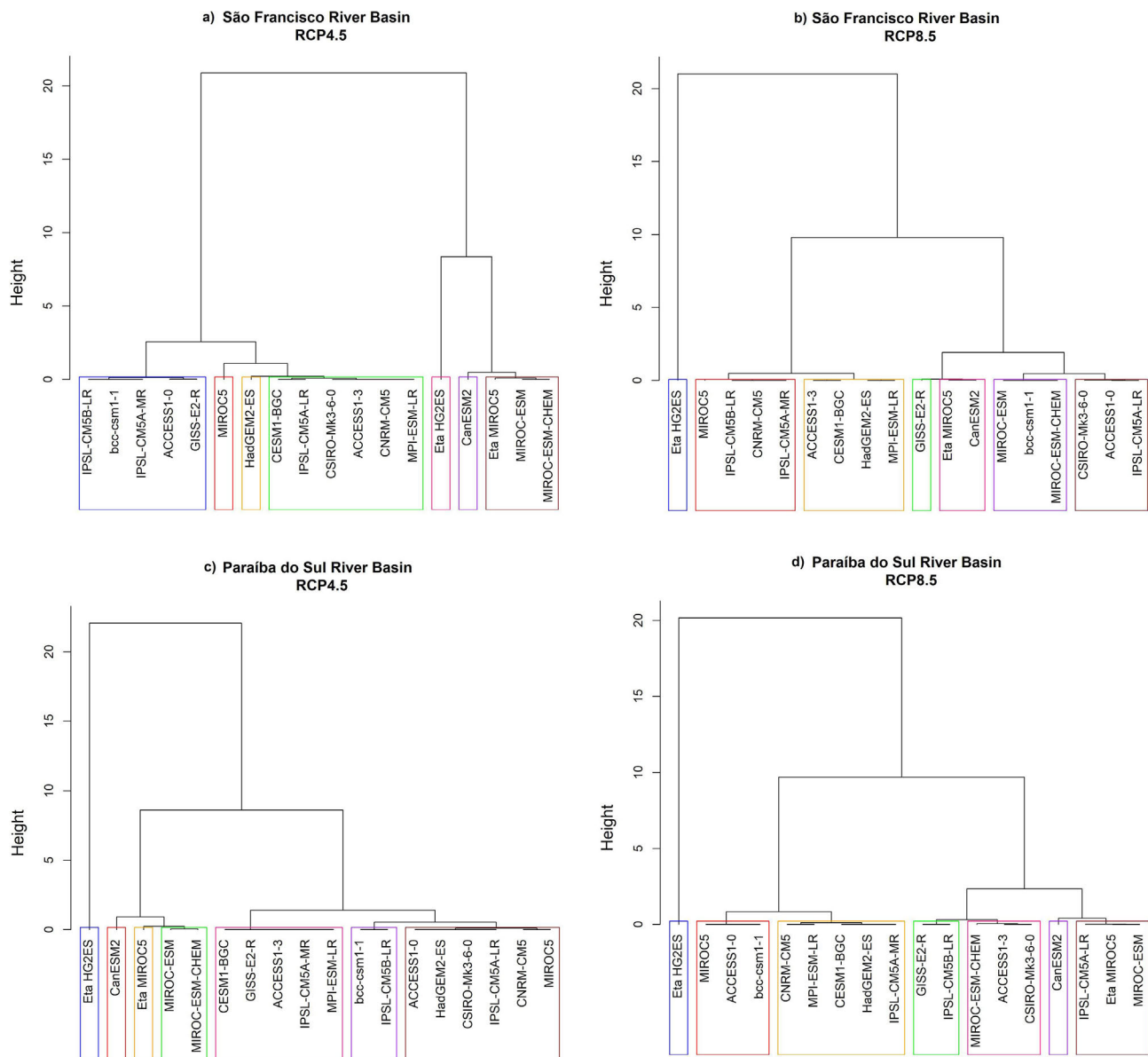


Figure 3 - Dendrogram showing the dissimilarity of the models for standardized data of the percentage anomaly of the mean annual precipitation in the São Francisco River basins (a) RCP4.5 (b) RCP8.5 and Paraíba do Sul (c) RCP4.5 (d) RCP8.5. The allocation of models for each cluster is indicated by colors.

more intense reductions in rainfall in the RCP8.5 scenario than in the RCP4.5 scenario in the short term for both basins how showed in Fig. 4. Considering both scenarios, most models indicated reductions in the São Francisco River basin. Precipitation anomalies of most GCMs models varied by up to -20% for the scenario with the lowest GHG emissions, with emphasis on the global model CanESM2. The regional models Eta-HadGEM2-ES and

Eta MIROC5 enhanced significant reductions in precipitation in both projections. It is interesting to note that the Eta-HadGEM2-ES model presented the highest magnitude of negative anomaly in both scenarios and among all models, with an emphasis on the RCP8.5 scenario, which presented a reduction of almost 40%.

In Paraíba do Sul, considering the RCP8.5 scenario, most GCM models indicated a decrease in precipitation in

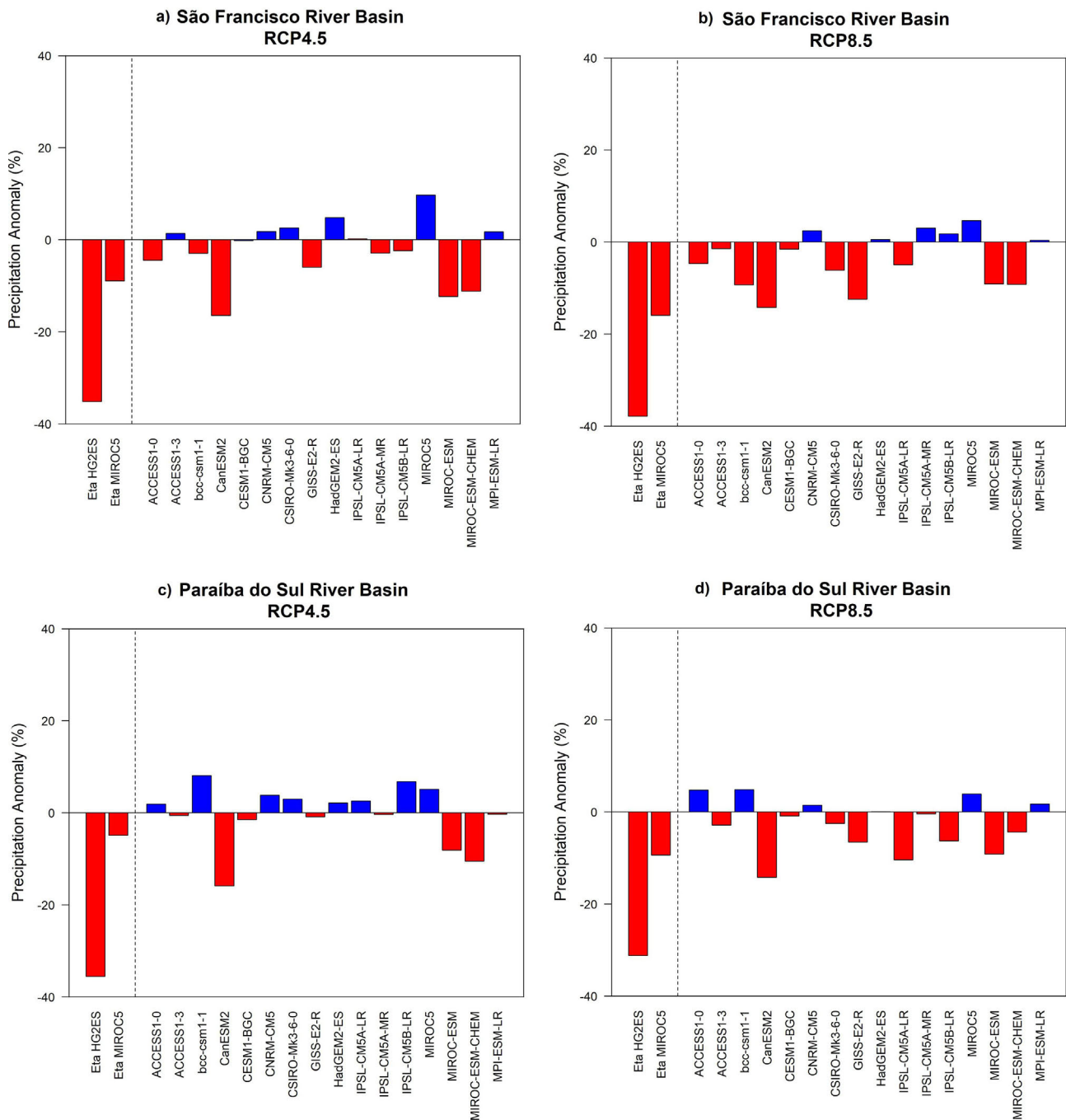


Figure 4 - Average annual precipitation anomaly (%) for the São Francisco River basins (a) RCP4.5 (b) RCP8.5 and Paraíba do Sul (c) RCP4.5 (d) RCP8.5 for the period 2011 to 2040.

the basin of just over 15%. Otherwise, in the scenario of lower GHG emissions, an increase in precipitation was pointed out, varying around 10%. The Eta-HadGEM2-ES model showed a more pronounced anomaly in this scenario when compared to the higher emission one. Again, this model showed the highest magnitude of negative anomaly in both scenarios and among all models.

The precipitation anomalies of the Eta model indicated that a large part of the basins may suffer from a great lack of rainfall in the period from 2011 to 2040, but it is important to highlight that when comparing the anomalies simulated by the two global models, HadGEM2-ES and MIROC5 with and without using the Eta regional model, it is evident that Eta tends to amplify the driest signal in the analyzed basins. Among the CMIP5 models, the CanESM2 model stood out in terms of negative percentage change. These results agree with those presented by Brasil (2015), in the previous study by Silveira *et al.* (2016) and in the work of Chou *et al.* (2017), in which the CanESM2 model showed a reduction in rainfall in the São Francisco for both scenarios. Brasil (2015) associates the intensification of negative precipitation anomalies, shown by the Eta regional model, to the increase in the temporal variability of the annual series in relation to global models.

The following figures show spatially the average percent precipitation anomaly of the climate models HadGEM2-ES and Eta-HadGEM2-ES (Fig. 5) and MIROC5 and Eta MIROC5 (Fig. 6) for scenarios RCP4.5 and RCP8.5 in the period 2011 to 2040 over the basins of the São Francisco and Paraíba do Sul Rivers.

The HadGEM2-ES global model showed a more pronounced increase in precipitation in most of the Paraíba do Sul and São Francisco River basins in the RCP4.5 scenario, mainly in the Sub-basin Médio São Francisco, with anomalies between 0 and 36% as shown in Fig. 5. In a more pessimistic scenario, its anomalies were more weakened, indicating percentages of increase of a maximum of 12% in part Médio and Sub-médio São Francisco and in part Paraíba do Sul. When used as a boundary condition for the Eta regional model, the model showed significant reductions in the entire Paraíba do Sul basin and in most of the São Francisco basin (except for part of the Sub-médio and Baixo São Francisco sub-basins). This decrease was greater in module for the RCP8.5 scenario, with magnitudes above 48%. This indicates the possibility of most of the analyzed basins becoming even drier.

In Fig. 6, a strong increase in precipitation of up to 24% was observed in most of the Paraíba do Sul Basin and throughout the São Francisco River basin, when compared to HadGEM2-ES (Fig. 5A and Fig. 5B), mainly in RCP4.5, with emphasis on the Baixo São Francisco sub-basin. Positive anomalies were identified in the two scenarios considered, attenuating their anomalies reaching only 12% in the most pessimistic scenario, mainly in a large part of the Médio São Francisco. For the Eta

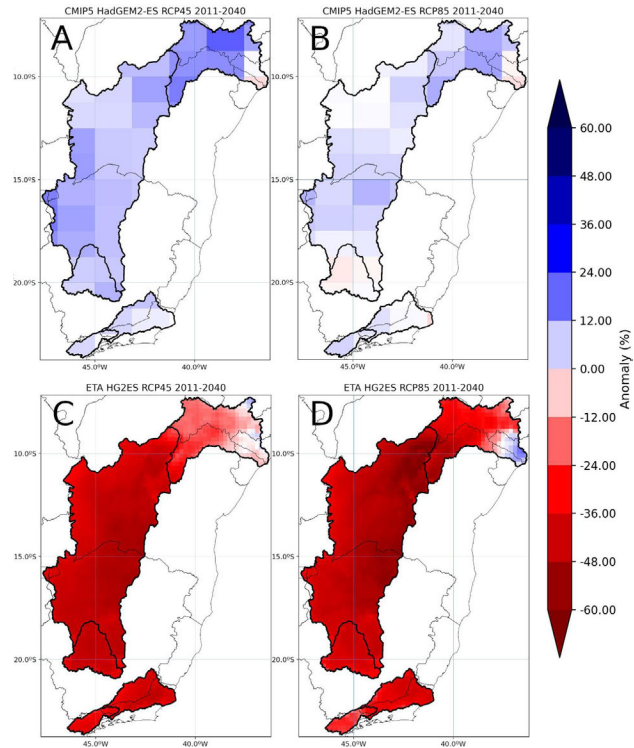


Figure 5 - Precipitation Anomaly for HadGEM2-ES models in scenarios A) RCP4.5 B) RCP8.5 and Eta-HadGEM2-ES in scenarios C) RCP4.5 D) RCP8.5 for the period from 2011 to 2040 over the São Francisco River basins and Paraíba do Sul.

MIROC5 model, significant reductions in precipitation were observed in most basins (except in the Sub-médio and Baixo São Francisco), and this decrease was also greater in module for the RCP8.5 scenario, up to 36% in relation to historical average. Considering the Sub-médio and Baixo São Francisco sub-basins, a great spatial divergence was observed in both scenarios regarding the anomaly signal, which, in turn, was significantly weakened in relation to the other regions.

4. Discussion

In the analysis of precipitation validation, the patterns of the Eta models and their global forcings showed a strong correlation with the observed data, especially for the Eta-HadGEM2-ES, HadGEM2-ES and MIROC5 models. Allied to this, the Eta-HadGEM2-ES showed the lowest standard deviation values in the two basins. This shows the good capacity of the simulations for the present climate of the Eta model nested to global models in reproducing the seasonality of rainfall in the São Francisco and Paraíba do Sul River basins.

As for seasonality, the observed data source showed a marked behavior with low variability from May to September for the São Francisco River basin, which may be associated with the dry period. In the Paraíba do Sul River

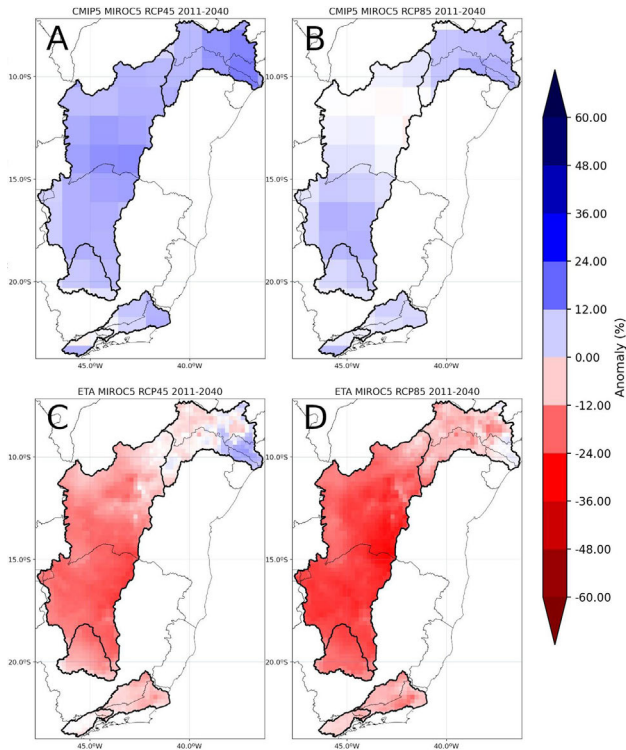


Figure 6 - Precipitation Anomaly for the MIROC5 models in scenarios A) RCP4.5 B) RCP8.5 and Eta MIROC5 in scenarios C) RCP4.5 D) RCP8.5 for the period 2011 to 2040 over the São Francisco and Paraíba River basins southern.

basin, a greater variability in terms of precipitation was identified when compared to the São Francisco River basin, even for the dry season. The highest median values were identified in December and January for São Francisco and Paraíba do Sul, respectively.

From the analysis of the dendrograms shown in Fig. 3, it was observed that models from the same institute tend to be grouped closer together and that a level of similarity was obtained very similar to the pairs of models that have much more common components - similar patterns were obtained in some studies from different parts of the globe (Mizuta *et al.*, 2014; Gibson *et al.*, 2017; Pathak *et al.*, 2019). The Eta-HadGEM2-ES model revealed a greater dissimilarity in terms of precipitation anomaly in relation to the other groups of models. Eta MIROC5 also showed a level of dissimilarity with respect to homogeneous groups, but established itself with the family of the MIROC-ESM/ESM-CHEM model set in most scenarios and basins. It is noteworthy that the dissimilarity identified between some sets of models from the same institution may be associated with changes in atmospheric components during the model development process (Pathak *et al.*, 2019).

The precipitation anomalies of the Eta model indicated that a large part of the basins may suffer from a great lack of rainfall in the period from 2011 to 2040, but

it is important to highlight that when comparing the anomalies simulated by the two global models, HadGEM2-ES and MIROC5 with and without using the Eta regional model, it is evident that Eta tends to amplify the driest signal in the analyzed basins. Among the CMIP5 models, the CanESM2 model stood out in terms of negative percentage change. These results agree with those presented by Brasil (2015), in the previous study by Silveira *et al.* (2016) and in the work of Chou *et al.* (2017), in which the CanESM2 model showed a reduction in rainfall in the São Francisco for both scenarios. Brasil (2015) associates the intensification of negative precipitation anomalies, shown by the Eta regional model, to the increase in the temporal variability of the annual series in relation to global models.

The fact that global climate models make use of different physical representations of processes, in a relatively low-resolution grid, introduces a certain degree of uncertainty in these future climate change scenarios and, consequently, in the assessment of vulnerability and impacts arising from it. Such uncertainties become greater in the case of regional models, as they are strongly dependent on the boundary conditions and the methods used to adapt the RCM variables to the lower spatial resolution of the GCM; thus, according to Pielke and Wilby (2012), large-scale weather errors in GCMs are not only absorbed by RCMs, but can be amplified, due to their higher spatial resolution. Furthermore, if the RCM is nested in just a few GCMs, the high-resolution scenarios do not cover the full range of projected changes that a larger number of GCMs would indicate as plausible futures, thus increasing the uncertainty of the results obtained (Hewitson *et al.*, 2014).

5. Conclusions

In order to better understand how the Eta regional model behaves in relation to some GCMs and, in particular, to its global forcings, this research compared a set of information for future climate change scenarios, in relation to its own forcing and to the other global models, in order to verify if there is an agreement of the Eta results with the GCM, assuming that the representation of the climate variable obtained from the RCMs presents a bias of intensification of its signal due to systematic errors. Obtaining more detailed projections for the analyzed regions, with a higher spatial resolution than that provided by a GCM, is of great use, particularly for studies of the impacts of climate change, aiding in the management and operation of water resources. Based on the results obtained, the main contributions of the study are:

- The strong correlation of the Eta model nested to the global models with observational data, showed the good ability to adequately represent the simulations for the present climate in reproducing the seasonality of rainfall in the São Francisco and Paraíba do Sul River

basins. It showed a greater variability when compared to the São Francisco River basin;

- Precipitation anomaly projections obtained from the Eta model indicated that a large part of the basins may suffer from a significant shortage of rainfall in the period 2011 to 2040 and mainly pointed to the disagreement in the signal of change with its GCMs and forcing other CMIP5 models. When comparing the anomalies simulated by the two global models, HadGEM2-ES and MIROC5, with and without the use of the regional model, it was evident that Eta amplifies the driest signal;
- This opposite sign between global models and when forced by regional model, may be related to the fact the Eta it is able to resolve local and mesoscale physical processes, which have more influence on precipitation. Since much of the dispersion identified in the results of the global models participating in the fifth IPCC report (AR5) for the Brazilian Northeast comes from their problems in satisfactorily resolving and reproducing the physical and dynamic processes that drive climate variability in the region, such as for example, ENSO and Tropical Atlantic variability (Bellenger *et al.*, 2014).
- The information generated suggests the need for a set analysis of models with different physical patterns, given that the use of information from only one model can neglect the uncertainty associated with climate change, which can reduce the robustness of the water resources management strategies adopted by not to consider all plausible scenarios. Especially for sectors that need information on a smaller spatial scale, such as water resources, agriculture, health, among others, decisions based on situations that disregard the uncertainty of the future climate can lead to strategies that are greatly regretted and affect their robustness.
- And finally, for further studies, it is necessary to discuss more carefully how the regional model is fed by the global one and how changes in the parameters of the regional model impact this divergence. In addition, given the computational cost and the existence of the need for more than one regional model to enable an analysis of climate projections, it is imperative that institutions evaluate the joint use of both dynamic downscaling and statistical downscaling. Although the last-mentioned technique has limitations, especially associated with stationarity. Given the points mentioned, the big question is not the reliability of the A or B result, but the treatment of uncertainty in the future climate that cannot be neglected, especially in such important sectors of society, such as water resources and the basins addressed in this work.

Acknowledgments

To the co-authors and to the Department of Hydraulic and Environmental Engineering (DEHA) of the Federal Uni-

versity of Ceará (UFC). This study was financed in part by the Coordenação de Aperfeiçoamento de Pessoal de Nível Superior - Brasil (CAPES) - Finance Code 001.

References

- ADAM, K.N.; FAN, F.M.; PONTES, P.R.M.; BRAVO, J.M.; COLLISCHONN, W. Mudanças climáticas e vazões extremas na Bacia do Rio Paraná. **Revista Brasileira de Recursos Hídricos**, v. 20, n. 4, p. 999-1007, 2015. doi
- ALVARES, C.A.S.; STAPE, J.L.; SENTELHAS, P.C.; MORAES, J.; LEONARDO; *et al.* Köppen's climate classification map for Brazil. **Meteorologische Zeitschrift**, v. 22, n. 6, p. 711-728, 2013. doi
- ARAKAWA, A.; LAMB, V.R. Computational design of the basic dynamical process of the UCLA general circulation model. **Methods Computational Physics**, v. 17, n. 1, p. 173-265, 1977. doi
- BEZERRA, B.G.; SILVA, L.L.; SANTOS E SILVA, C.M.; CARVALHO, G.G. Changes of precipitation extremes indices in São Francisco River Basin, Brazil from 1947 to 2012. **Theor Appl Climatol**, v. 135, n. 1-2, p. 565-576, 2019. doi
- BLACK, T.L. The new NMC mesoscale Eta model: Description and forecast examples. **Wea. and Forecasting**, v. 9, n. 2, p. 265-278, 1994. doi
- BRASIL. **Brasil 2040: Resumo Executivo**. Brasília: Secretaria de Assuntos Estratégicos, 2015.
- BRASIL. **Modelagem Climática e Vulnerabilidades Setoriais à Mudança do Clima no Brasil**. Brasília: Ministério da Ciência, Tecnologia e Inovação, 2016.
- BELLENGER, H.; GUILYARDI, E.; LELOUP, J.; LENGAINNE, M.; VIALARD, J. ENSO representation in climate models: From CMIP3 to CMIP5. **Clim Dyn**, v. 42, n. 7-8, p. 1999-2018, 2014. doi
- BRITO, A.L.; VEIGA, J.A.P.; CORREIA, F.W.; CAPISTRANO, V.B. Avaliação do desempenho dos modelos HadGEM2-ES e Eta a partir de indicadores de extremos climáticos de precipitação para a Bacia Amazônica. **Revista Brasileira de Meteorologia**, v. 34, n. 32, p. 165-177, 2019. doi
- BORGES DE AMORIM, P.; CHAFFE, P.B. Towards a comprehensive characterization of evidence in synthesis assessments: the climate change impacts on the Brazilian water resources. **Climatic Change**, v. 155, n.1, p. 37-57, 2019. doi
- CBHSF, Comitê da Bacia Hidrográfica do Rio São Francisco. **Plano de Recursos Hídricos da Bacia Hidrográfica do Rio São Francisco 2016-2025**. Alagoas: CBHSF, 2016.
- CHEN, T.H.; HENDERSON-SELLERS, P.C.D.; MILLY, A.J.; PITMAN, A.C.M.; BELJAARS, J. *et al.* Cabauw experimental results from the Project for Intercomparison of Land-Surface Parameterization Schemes. **J. Climate**, v. 10, n. 6, p. 1194-1215, 1997. doi
- CHOU, S.C.; MARENGO, J.A.; LYRA, A.A.; SUEIRO, G.; PESQUERO, J.F.; *et al.* Downscaling of South America present climate driven by 4-Member HadCM3 runs. **Climate Dynamics**, v. 38, n.3-4, p. 635-653, 2012. doi
- CHOU, S.C.; LYRA, A.; MOURÃO, C.; DERECZYNSKI, C.; PILOTTO, I. *et al.* Evaluation of the Eta simulations nested

- in three global climate models. **American Journal of Climate Change**, v. 3, n. 5, p. 438-454, 2014. [doi](#)
- CHOU, S.C.; LYRA, A.A.; CHAGAS, D.J.; SUEIRO, G.; GOMES, J.L.; *et al.* Projeções de mudanças de precipitação na Bacia do Rio São Francisco. In: **20 Simpósio Brasileiro de Recursos Hídricos**, Florianópolis, p. 1-8, 2017.
- COLLINS, W.J.; BELLOUIN, N.; DOUTRIAUX-BOUCHER, M.; GEDNEY, N.; HALLORAN, P. Development and evaluation of an earth system Model-HadGEM2. **Geoscientific Model Development**, v. 4, n. 4, p. 1051-1075, 2011. [doi](#)
- COX, P.M. **Description of the "TRIFFID" dynamic global vegetation model**. UK: Met Office, 2001.
- CRUZ, M.; MOTA, P.; ARAGÃO, R.; FRANCA ROCHA, R. Avaliação das precipitações geradas pelo modelo climático regional ETA-HadGEM2-ES para o estado de Sergipe. **Scientia Plena**, v. 13, 109913, 2017. [doi](#)
- DERECZYNSKI, C.; CHOU, S.C.; LYRA, A.; SONDERMANN, M.; REGOTO, P. Downscaling of climate extremes over South America - Part I: Model evaluation in the reference climate. **Weather and Climate Extremes**, v. 29, 100273, 2020. [doi](#)
- DI LUCA, A.; DE ELÍA, R.; LAPRISE, R. Potential for added value in precipitation simulated by high-resolution nested regional climate models and observations. **Clim. Dyn.** v. 38, n.5-6, p. 1229-1247, 2012. [doi](#)
- FARIAS, C.W.L.A.; MONTENEGRO, S.M.G.L.; LINS, F.C.A.; MONTENEGRO, A.A.A. Correção de tendência das projeções climáticas futuras simuladas pelo modelo regional EtaHadgem2-Es para a Bacia Hidrográfica do Rio Mundaú, Nordeste do Brasil. **Journal of Environmental Analysis and Progress**, v. 5, n. 3, p. 288-301, 2020. [doi](#)
- FELS, S.B.; SCHWARZKOPF, M.D. The simplified exchange approximation: A new method for radiative transfer calculations. **Journal of the Atmospheric Sciences**, v. 32, n. 7, p. 1475-1488, 1975. [doi](#)
- FOX, D.G. Judging air quality model performance. **Bull. Am. Meteorol. Soc.**, v. 62, n. 5, p. 599-609, 1981. [doi](#)
- GADD, A.J. A split-explicit integration scheme for numerical weather prediction. **Quarterly Journal of the Royal Meteorological Society**, v. 104, n. 441, p. 569-582, 1978. [doi](#)
- GIBSON, P.B.; PERKINS-KIRKPATRICK, S.E.; ALEXANDER, L.V.; FISCHER, E.M. Comparing Australian heat waves in the CMIP5 models through cluster analysis. **J. Geophys. Res. Atmos.**, v. 122, n. 6, p. 3266-3281, 2017. [doi](#)
- GIORGI, F. Thirty years of regional climate modeling: Where are we and where are we going next? **Journal of Geophysical Research: Atmospheres**, v. 124, n. 11, p. 5696-5723, 2019. [doi](#)
- HASUMI, H. **CCSR Ocean Component Model (COCO), Version 4.0**. Tokyo: Centre for Climate System Research, 2007.
- HEWITSON, B.C.; DARON, J.; CRANE, R.G.; ZERMOGLIO, M.F.; JACK, C. Interrogating empirical-statistical downscaling. **Climatic Change**, v. 122, n. 4, p. 539-554, 2014. [doi](#)
- INTERGOVERNMENTAL PANEL ON CLIMATE CHANGE (IPCC). **Climate Change 2013: The Physical Science Basis. Contribution of Working Group I to the Fifth Assessment Report of the Intergovernmental Panel on Climate Change**. Cambridge: Cambridge University Press, 2013.
- JACKSON, I.J.; WEINAND, H. Classification of tropical rainfall stations: A comparison of clustering techniques. **International Journal of Climatology**, v. 15, n. 9, p. 985-994, 1995. [doi](#)
- JANJIC, Z. I. The step-mountain Eta coordinate model: Further developments of the convection, viscous sublayer, and turbulence closure schemes. **Monthly Weather Review**, v. 122, n. 5, p. 927-945, 1994. [doi](#)
- JOLLIFFE, I.; STEPHENSON, D. **Forecast Verification: A Practitioner's Guide in Atmospheric Science**. UK: John Wiley and Sons, 2003.
- LACIS, A.A.; HANSEN, J.E. A parameterization of the absorption of solar radiation in earth's atmosphere. **Journal of the Atmospheric Sciences**, v. 31, n. 1, p. 118-133, 1974. [doi](#)
- LYRA, G.B.; GARCIA, B.I.L.; PIEDADE, S.M.S.; SEDIYAMA, G.C.; SENTELHAS, P.C. Regiões homogêneas e funções de distribuição de probabilidade da precipitação pluvial no estado de Táchira, Venezuela. **Pesquisa Agropecuária Brasileira**, v. 41, n. 2, p. 202-215, 2006. [doi](#)
- LYRA, G.; OLIVEIRA-JÚNIOR, J.; ZERI, M. Cluster analysis applied to the spatial and temporal variability of monthly rainfall in Alagoas state, Northeast of Brazil. **International Journal of Climatology**, v. 34, n. 13, p. 3546-3558, 2014. [doi](#)
- MARENGO, J.A.; CHOU, S.C.; KAY, G.; ALVES, L.M.; PESQUERO, J.F. *et al.* Development of regional future climate change scenarios in South America using the Eta CPTEC/HadCM3 climate change projections: Climatology and regional analyses for the Amazon, São Francisco and the Parana River Basins. **Climate Dynamics**, v. 38, n. 9-10, p. 1829-1848, 2012. [doi](#)
- MARTIN, G.M.; BELLOUIN, N.; COLLINS, W.J.; CULVERWELL, I.D.; HALLORAN, P.R. *et al.* The HadGEM2 family of Met Office Unified Model climate configurations. **Geoscientific Model Development**, v. 4, n. 3, p. 723-757, 2011. [doi](#)
- MELLOR, G.L.; YAMADA, T. A hierarchy of turbulence closure models for boundary layers. **Journal of the Atmospheric Sciences**, v. 31, n. 7, p. 1791-1806, 1974. [doi](#)
- MESINGER, F. A blocking technique for representation of mountains in atmospheric models. **Rivista di Meteorologia Aeronautica**, v. 44, n. 1-4, p. 195-202, 1984.
- MESINGER, F.; JANJIC, Z.; SLOBODAN, N.; ZUPANSKI, D.; DEAVEN, D. The step-mountain coordinate: Model description and performance for cases of Alpine Lee Cyclogenesis and for a Case of an Appalachian Redevelopment. **Mon. Wea. Rev.**, v. 116, n. 7, p. 1493-1518, 1988. [doi](#)
- MIZUTA, R.; ARAKAWA, O.; OSE, T.; KUSUNOKI, S.; ENDO, H. *et al.* Classification of CMIP5 future climate responses by the tropical sea surface temperature changes. **SOLA**, v. 10, n. 1, p. 167-171, 2014. [doi](#)
- MOISE, A.; WILSON, L.; GROSE, M.; WHETTON, P.; WATTERSON, I.G. *et al.* Evaluation of CMIP3 and CMIP5 models over the Australian Region to inform confidence in

- projections. **Australian Meteorological and Oceanographic Journal**, v. 65, n. 1, p.19-53, 2015. doi
- MOORE, D.S. **The Basic Practice of Statistics**. New York: W.H. Freeman, 2007.
- MOURA, A.D.; SHUKLA, J. On the dynamics of drought in Northeast Brazil: Observations, theory and numerical experiments with a general circulation model. **Journal of Atmospheric Research**, v. 38, n. 12, p. 2653-2675, 1981. doi
- NOBRE, P. **Variabilidade climática sobre o Atlântico Tropical parte II: Estudo de casos**. São José dos Campos: INPE, 1994.
- OLIVEIRA, V.A.; MELLO, C.R.; VIOLA, M.R.; SRINIVASAN, R. Assessment of climate change impacts on streamflow and hydropower potential in the headwater region of the Grande River basin, Southeastern Brazil. **International Journal of Climatology**, v. 37, n. 15, p. 5005-5023, 2017. doi
- PAINEL BRASILEIRO DE MUDANÇAS CLIMÁTICAS (PBM). **Base científica das mudanças climáticas. Contribuição do Grupo de Trabalho 1 do Painel Brasileiro de Mudanças Climáticas ao Primeiro Relatório da Avaliação Nacional sobre Mudanças Climáticas**. Rio de Janeiro: COPPE, 2014.
- PAINEL BRASILEIRO DE MUDANÇAS CLIMÁTICAS (PBM). **Mudanças Climáticas e Cidades. Relatório Especial do Painel Brasileiro de Mudanças Climáticas**. Rio de Janeiro: COPPE, 2016.
- PATHAK, R.; SAHANY, S.; MISHRA, S.K.; DASH, S.K. Precipitation biases in CMIP5 Models over the South Asian region. **Sci. Rep.**, v. 9, 9589, 2019. doi
- PEREIRA, D.P.; SOUZA LIMA, J.S.; XAVIER, A.C.; PASSOS, R.R.; FIEDLER, N.C. Aplicação do diagrama de Taylor para avaliação de interpoladores espaciais em atributos de solo em cultivo com eucalipto. **Revista Árvore**, v. 38, n. 5, p. 899-905, 2014. doi
- PIANI, C.; HAERTER, J.O.; COPPOLA, E. Statistical bias correction for daily precipitation in regional climate models over Europe. **Theoretical and Applied Climatology**, v. 99, n. 1-2, p. 187-192, 2010. doi
- PICKLER, C.; MÖLG, T. General circulation model selection technique for downscaling: Exemplary application to East Africa. **Journal of Geophysical Research: Atmospheres**, v. 126, e2020JD033033, 2021. doi
- PIELKE, R.A.; WILBY, R.L. Regional climate downscaling: What's the point? **Eos Trans. AGU**, v. 93, n. 5, p. 52-53, 2012. doi
- RUMMUKAINEN, M. Added value in regional climate modeling. **WIREs Climate Change**, v. 7, n. 1, p. 145-159, 2016. doi
- SALES, D.C.; COSTA, A.A.; SILVA, E.M.; VASCONCELOS JÚNIOR, F.C.; CAVALCANTE, A.M.B.; *et al.* Projeções de mudanças na precipitação e temperatura no Nordeste brasileiro utilizando a técnica de downscaling dinâmico. **Revista Brasileira de Meteorologia**, v. 30, n. 4, p. 435-456, 2015. doi
- SCHNEIDER, U.; BECKER, A.; FINGER, P.; MEYER-CHRISTOFFER, A.; RUDOLF, B.; *et al.* **GPCC Full Data Reanalysis Version 6.0 at 0.5°: Monthly Land-Surface Precipitation from Rain-Gauges Built on GTS-Based and Historic Data**. Disponível em https://opendata.dwd.de/climate_environment/GPCC/html/fulldata_v6_doi_download.html, acesso em 08 de jun. 2021.
- SEKIGUCHI, M.; NAKAJIM, T. A k-distribution-based radiation code and its computational optimization for an atmospheric general circulation model. **Journal of Quantitative Spectroscopy and Radiative Transfer**, v. 109, n. 17-18, p. 2779-2793, 2008. doi
- SILVA, J.G.; WANDERLEY, H.S.; SANTOS, E.O.; LYRA, G.B. Avaliação e correção das simulações do modelo Eta/CPTEC - HADCM3 para o estado do Rio de Janeiro. **Revista Brasileira de Geografia Física**, v. 13, p. 350-363, 2020. doi
- SILVA, M.V.M.; SILVEIRA, C.S.; SILVA, G.K.; PEDROSA, W.H.; VASCONCELOS, A.D.; *et al.* Projections of climate change in streamflow and affluent natural energy in the Brazilian hydroelectric sector of CORDEX models. **Revista Brasileira de Recursos Hídricos**, v. 25, e34, 2020. doi
- SILVEIRA, C.S.; SOUZA FILHO, F.A.; MARTINS, E.S.P.R.; OLIVEIRA, J.L.; COSTA, A.C.; *et al.* Mudanças climáticas na bacia do rio São Francisco: Uma análise para precipitação e temperatura. **Revista Brasileira de Recursos Hídricos**, v. 21, n. 2, p. 416-428, 2016. doi
- SOLMAN, S.A. Regional climate modeling over South America: A review. **Advances in Meteorology**, v. 2013, 504357, 2013. doi
- TAKATA, K.; EMORI, S.; WATANABE, T. Development of the minimal advanced treatments of surface interaction and runoff. **Global and Planetary Change**, v. 38, n. 1-2, p. 209-222, 2003. doi
- TAYLOR, K.E. Summarizing multiple aspects of model performance in a single diagram. **Journal of Geophysical Research**, v. 106, n. 7, p. 7183-7192, 2001. doi
- TAYLOR, K.; RONALD, S.T.; MEEHL, G. An overview of CMIP5 and the experiment design. **Bulletin of the American Meteorological Society**, v. 93, n. 4, p. 485-498, 2011. doi
- TEUTSCHBEIN, C.; SEIBERT, J. Regional climate models for hydrological impact studies at the catchment scale: A review of recent modeling strategies. **Geography Compass**, v. 4, n. 7, p. 834-860, 2010. doi
- TEJADAS, B.E.; BRAVO, J.M.; SANAGIOTTO, D.G.; TASSI, R.; MARQUES, D.M.L. Projeções de vazão afluente à lagoa mangueira com base em cenários de mudanças climáticas. **Revista Brasileira de Meteorologia**, v. 31, n. 3, p. 262-272, 2016. doi
- VALÉRIO, E.; FRAGOSO JÚNIOR, C. Avaliação dos efeitos de mudanças climáticas no regime hidrológico da bacia do rio Paraguaçu, BA. **Revista Brasileira de Recursos Hídricos**, v. 20, n. 4, p. 872-887, 2015. doi
- VAN VUUREN, D.; EDMONDS, J.; KAINUMA, M.; RIAHI, K.; THOMSON, A.; *et al.* The representative concentration pathways: An overview. **Climatic Change**, v. 109, n. 1, p. 5-31, 2011. doi
- WARD, J.H. Hierarchical grouping to optimize an objective function. **Journal of the American Statistical Association**, v. 58, n. 301, p. 236-244, 1963. doi

- WATANABE, M.; SUZUKI, T.; O'ISHI, R.; KOMURO, Y.; WATANABE, S.; *et al.* Improved climate simulation by MIROC5: Mean states, variability, and climate sensitivity. **Journal of Climate**, v. 23, n. 23, p. 6312-6335, 2010. [doi](#)
- WILKS, D.S. **Statistical Methods in the Atmospheric Sciences**. London: Academic Press, 2019.
- ZÁKHIA, E.M.S.; ALVARENGA, L.A.; TOMASELLA, J.; MARTINS, M.A. Avaliação de projeções climáticas para uma bacia experimental, localizada na região sul de Minas Gerais. **Revista Ibero Americana de Ciências Ambientais**, v. 11, n. 6, p. 234-250, 2020. [doi](#)

Internet Resources

CEIVAP, Comitê de Integração da Bacia Hidrográfica do Rio Paraíba do Sul, <http://www.ceivap.org.br>.



License information: This is an open-access article distributed under the terms of the Creative Commons Attribution License (type CC-BY), which permits unrestricted use, distribution and reproduction in any medium, provided the original article is properly cited.